Bulk Power System Dynamics and Control V, August 26-31, 2001, Onomichi, Japan

# Evaluation of reactive power reserves with respect to contingencies

F. Capitanescu T. Van Cutsem*

University of Liège, Dept. of Electrical Engineering
Montefiore Institute, Sart-Tilman B37, B-4000 Liège, Belgium
vct@montefiore.ulg.ac.be

## 1. Introduction

Following a disturbance, most generators, synchronous condensers and static var compensators of a power system react to maintain their voltages at (almost) constant values, by producing more reactive power. This is possible as long as no physical limit prevents this additional reactive power from being produced. When such limits are encountered, transmission voltages fall down more or less progressively, until instability occurs either in the form of a loss of synchronism (insufficient voltage support to transfer active power over long distances) or a voltage instability at the load ends (inability of the transmission and generation system to meet the load demand) [1, 2].

Reactive reserves are thus necessary for both angle and voltage stability. Although this paper focuses on the second aspect, the proposed method can be used in a more general context.

It is rather easy to compute or measure the individual reactive reserve available on the above components. However, it is well-known that reactive power cannot be transmitted over long distances. For instance, remote generators cannot provide a significant voltage support. Even if a generator has a large reserve with respect to its physical limit, its effective ability to help containing remote incidents may be limited. In other words, in large systems, reactive reserves cannot be obtained by merely summing up individual reserves.

Although the above facts are well known, there is no clear method to evaluate reactive power reserves with respect to a contingency.

Reference [3] proposed to monitor reactive margins on voltage zones in order to assess the voltage profile quality. A voltage zone is defined as a group of "tightly coupled" generator buses, together with the union of the sets of load buses that they mutually support. The voltage zone margin is the difference between: (i) the zone reserve, obtained by adding the individual reserves of generators within the zone, and (ii) the additional reactive generation needed to maintain acceptable voltage levels after any given contingency. The partition of the system into zones relies on load flow sensitivity information.

References [4, 5] rely on the notion of voltage control area, defined as the set of load and generator buses whose voltages respond "coherently" to outside changes in reactive load and generation. The "reactive reserve basin" of the area is then defined as the sum of the reactive reserves exhausted at the minimum of the VQ curve [1, 2] relative to any bus of the area. The percentage of basin reactive reserve remaining after a disturbance is used as a measure of proximity to voltage instability.

As long as the above voltage (control) areas are identified from sensitivity analysis of a pre-contingency configuration, their validity may be questioned when seeking reserves with respect to instability (not just voltage profile quality) and severe contingencies.

Two methods for determining the "effective" reactive reserve of a specific voltage area are outlined in [6]. The first method relies on VQ curves determined at one bus or for one area. The reserve is taken as the sum of individual reserves of the generators under limit at the minimum of the curve. It is thus an image, on the generation side, of a particular load power margin. The second method computes an effective power reserve as the weighted sum of individual reserves; the weights are based on sensitivities of generator reactive outputs to reactive loads.

The evaluation of reactive power reserves has gained attention within the context of unbundling of generation and tranmission. Provision of reactive power reserve is an ancillary service that has to be valuated and paid accordingly. The value of this service must be assessed with respect to the capability of helping the system to face incidents.

To valuate individual reactive reserves, Ref. [7] proposes an "equivalent reactive compensation" method. The latter consists of adding fictitious synchronous condensers at all or selected load buses, and switching all reactive sources under constant power. The synchronous condenser outputs are monitored while the production of each source is varied from base case to maximum capability. This provides a basis for comparing the relative efficiencies of the various sources. Note, however, that tranferring voltage control from the generation to the load side results in a fundamental change of system behaviour: load flow divergence, overvoltage and unusual sensitivities problems can be experienced. The proper location of the synchronous condensers is

* Research Director FNRS (National Funds for Scientific Research, Belgium)

a key step in this method, to avoid abnormal operating conditions and obtain meaningful results.

This paper is organized as follows. Section 2 proposes definitions of respectively the effective capability of a generator, the minimal reactive reserve to face a contingency and the corresponding current value. A simple computational procedure is described in Section 3. Section 4 deals with examples, obtained on a simple test and a real-life system, respectively. Conclusion is offered in Section 5.

## 2. Towards a definition of reactive reserves

### *2.1. Effective capability of generators*

Consider the simple 3-bus system of Fig. 1. In this system, the load at bus L is fed by generator 1, electrically close to bus L, and generator 2, located farther away (the lines in Fig. 1 represent both step-up transformers and transmission lines).

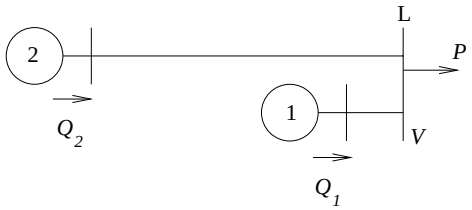

Figure 1: Simple 3-bus system

We denote the generator reactive power capabilities by $Q_1^{lim}$ and $Q_2^{lim}$, respectively. As is well-known, these limits are mainly dictated by the thermal overload capability of the field or armature winding, as depicted by the machine capability curves [1, 2].

Figure 2.a shows the PV curve relating the load voltage $V$ to the load active power $P$. The load is assumed to increase under constant power factor and the two generators respond to the active demand increase according to some participation factors. The breakpoint B corresponds to the loss of voltage control by generator 1, under the action of an overexcitation (or, possibly, a stator current) limiter. $P^{max}$ is the maximum power that can be delivered to the load by the combined generation/transmission system.

The reactive power response of each generator is considered in Fig. 2.b. Under the effect of reactive power losses, both productions increase more than linearly. As long as it controls its voltage, generator 1, located closer to the load, is more responsive, as indicated by the higher slope of the $Q_1$ vs. $P$ curve. For simplicity, we assume that, once under limit, generator 1 has a constant reactive power output $Q_1^{lim}$ (this simplifying assumption is not needed by the method described in Section 3). When the system operates above $P = P_B$, the whole reactive power has to come from the farther generator 2. Hence, the slope of the $Q_2$ vs. P curve increases suddenly when passing through point B. At the loadability limit $P = P^{max}$, this curve has an infinite slope, a well-known characteristic of saddle-node bifurcations [2].

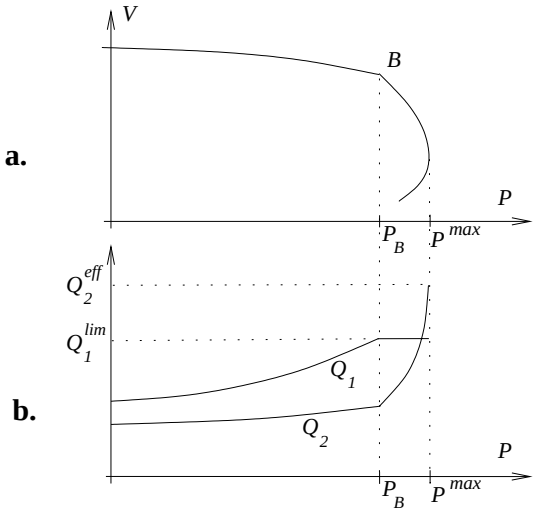

Figure 2: PV and PQ curves of the 3-bus system

Let $Q_2^{eff}$ be the reactive production of generator 2 at the loadability limit. We call this value the *effective reactive limit* of generator 2, as opposed to the *technical limit* $Q_2^{lim}$. For generator 1, which produces $Q_1^{lim}$ at the bifurcation point, both limits coincide. For generator 2, on the other hand, transmission system constraints prevent from taking advantage of $Q_2^{lim} - Q_2^{eff}$ Mvars, at least when load is increased at bus L.

The total reactive reserve with respect to the effective capabilities is given by:

$$R = (Q_1^{eff} - Q_1) + (Q_2^{eff} - Q_2)$$

Clearly, this reserve decreases as the load increases and vanishes at the loadability limit point, i.e.

$$R \to 0 \quad \text{when} \quad P \to P^{max} \tag{1}$$

What has been said applies to all reactive power sources. We will continue speaking of generators but the proposed definition and method apply to synchronous condensers and static var compensators as well.

### *2.2. Reactive reserves with respect to a contingency*

Consider a power system with $n$ generators in service. We denote by $Q_i$ the reactive production of the $i$-th generator ($i = 1, \ldots, n$) at the current operating point and by $Q_i^{lim}$ its reactive capability.

Following a contingency, most controlled reactive power sources react by increasing their production in order to keep their controlled voltages (almost) constant. In other words, the contingency will "consume" some of the reactive power reserve available on generators. We know that the farther the generator, the lower its support. Hence, the question: *out of the total reserve*

$\sum_i Q_i^{lim} - Q_i$, *how much is needed and on which generators, in order the system to respond to the contingency in an acceptable way ?*

Whether the system response to a contingency is acceptable must be defined with respect to appropriate criteria. At least, voltage stability is required, but in addition to being stable, the system might be requested to meet some operating constraints.

The approach followed in this paper consists in stressing the system in its pre-contingency configuration, until reaching an unacceptable post-contingency response. A simple analysis of the last acceptable situation will provide us with the sought information, as explained hereafter.

The system stress considered here consists of changes in bus power injections which make the system weaker by increasing power transfer over relatively long distances and/or drawing on reactive power reserves. Namely, at the $i$-th bus, the load active power $P_{li}$, the load reactive power $Q_{li}$ or the generator active power $P_{gi}$ vary according to:

$$P_{li} = P_{li}^o + \lambda_{li}\, S \quad (2)$$

$$Q_{li} = Q_{li}^o + \mu_{li}\, S \quad (3)$$

$$P_{gi} = P_{gi}^o + \lambda_{gi}\, S \quad (4)$$

where $P_{li}^o$, $Q_{li}^o$ and $P_{gi}^o$ are the corresponding base case values, $S$ is a scaling factor, and $(\lambda_{li}, \mu_{li}, \lambda_{gi})$ are participation factors. Typical stresses consist of increasing load in an area A and generation in a remote area B ($\lambda_{li}, \mu_{li} > 0, i \in A; \lambda_{gj} > 0, j \in B$) or decreasing generation in an area A and increasing generation in a remote area B ($\lambda_{gi} < 0, i \in A; \lambda_{gj} > 0, j \in B$).

Let $S^\star$ be the maximum stress such that the system responds in an acceptable way to the contingency. We denote by:
• $Q^\star_{pre,\,i}$ the reactive power production of the $i$-th generator in the pre-contingency configuration, after the system has been stressed at the critical level $S^\star$
• $Q^\star_{post,\,i}$ the reactive power production of the same generator in the post-contingency situation, for the same level of stress.

Since $S^\star$ is such that the system response is marginally acceptable after the contingency has occurred, we consider $Q^\star_{post,\,i}$ as the effective capability of the $i$-th generator. Similarly to what was said in Section 2.1 for a load increase :
• any additional Mvar available on this machine cannot be used to face the contingency in an acceptable way;
• in this particular post-contingency state, some generators may be at their limits while others may still have some reserve. For the latter the effective capability is smaller than the technical one, while for the former both limits coincide.

Thus, the minimal reactive reserve needed to face the contingency with an acceptable response is given by:

$$R^{min} = \sum_{i=1}^{n} Q^\star_{post,\,i} - Q^\star_{pre,\,i} \quad (5)$$

Now, those generators not involved in (e.g. located far away from) the contingency are characterized by:

$$Q^\star_{post,\,i} \simeq Q^\star_{pre,\,i} \quad (6)$$

and hence, will not significantly contribute to the above sum. In practice, we identify the set of generators involved in the contingency as:

$$\mathcal{E} = \{i : Q^\star_{post,\,i} - Q^\star_{pre,\,i} > \epsilon\} \quad (7)$$

where $\epsilon$ is a tolerance. Thus, for a small enough $\epsilon$, we have:

$$R^{min} \simeq \sum_{i \in \mathcal{E}} Q^\star_{post,\,i} - Q^\star_{pre,\,i} \quad (8)$$

This formulation conveys a bit more information in the sense that it focuses on generators playing a significant role.

The corresponding reserve at an operating point characterized by productions $Q_i$ is given by:

$$R = \sum_{i \in \mathcal{E}} Q^\star_{post,\,i} - Q_i \quad (9)$$

Note that generators not involved in the contingency may respond to the stress and hence be characterized by:

$$Q^\star_{pre,\,i} > Q_i$$

or, taking (6) into account:

$$Q^\star_{post,\,i} > Q_i$$

Hence, extending the sum in (9) over all generators would include in reserve $R$ a significant contribution from generators that do not respond to the contingency. Therefore, it is essential to restrict the summation in (9) to the set $\mathcal{E}$ only. Unless otherwise specified, we will use the corresponding formula (8) for the minimal reserve, for the sake of symmetry.

Finally, note that there is a risk of not including a significant generator in the $\mathcal{E}$ set, if: (i) it approaches its (technical) limit by less than $\epsilon$ in the stressed pre-contingency situation, and (ii) hits its limit after the contingency. In this case, one can re-simulate the contingency, at the stress level $S^\star$, with the limit removed. If the "freed" generator responds by more than $\epsilon$ to the contingency, it is included in $\mathcal{E}$.

### *2.3. A security index*

It follows from the above derivation that:

$$R \to R^{min} \quad \text{when} \quad S \to S^\star \quad (10)$$

which is an extension of (1) including the contingency effect. In fact, (1) can be seen as a particular case of (10) for an infinitely mild disturbance that can be faced without reactive reserve, i.e. $R^{min} = 0$.

Clearly, the system is secure with respect to the contingency as long as:

$$R > R^{min}$$

or in dimensionless form:

$$I = \frac{R - R^{min}}{R^{min}} > 0 \qquad (11)$$

The larger the index I, the higher the system robustness with respect to the contingency of concern.

The above indices depend to some extent on the stress chosen to push the system towards its limits. This aspect is further discussed in Section 4.2.

## 3. Computational procedure

The determination of $R^{min}$ and $R$ relies on $Q^{\star}_{pre,\,i}$ and $Q^{\star}_{post,\,i}$ which in turn require to determine $S^{\star}$, the maximum pre-contingency stress such that the system responds in an acceptable way to the contingency.

This can be done using the simple and robust binary search algorithm. The latter consists of building a smaller and smaller interval $[S_\ell \;\; S_u]$, where $S_\ell$ corresponds to a stable post-contingency evolution and $S_u$ to an unstable one, until $S_u - S_\ell$ becomes lower than a tolerance $\Delta$. The search starts with $S_\ell = 0$ and $S_u = S_{max}$, a maximum stress of interest. At each step, the interval is divided in two equal parts; if the midpoint is found stable (resp. unstable) it is taken as the new lower (resp. upper) bound. The final value of $S_\ell$ is the sought stress $S^{\star}$. The procedure is sketched in Fig. 3, where the dashed arrows show the sequence of tested stress levels.

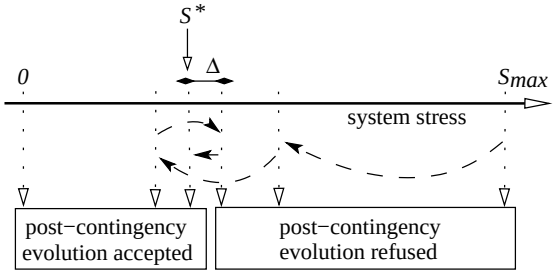


Figure 3: Binary search of $S^{\star}$

Different tools can be thought of to evaluate the system response, ranging from post-contingency load flows to full time-scale simulations. In this work we have used the fast time-domain Quasi Steady-State (QSS) approach which offers a good compromize between accuracy and efficiency [8, 2, 9].

Note that binary searches are also used to compute secure operation limits with respect to contingencies [9]. In this context, the reactive reserves are obtained at no cost as a by-product of the limit search. In some sense, the index $I$ is an alternative way of presenting results, looking from the generator side. In addition, it brings complementary information on the generators responsible for unacceptable voltage profiles.

## 4. Illustrative examples

### *4.1. Examples from the Nordic 32 test system*

We consider the 80-bus, 23-generator system shown in Fig. 4, a variant of the "Nordic 32" system used e.g. by CIGRE Task Force 32.02.08 on Long-Term Dynamics (1995). A rather heavy power transfer takes place from the "North" to the "South" area.

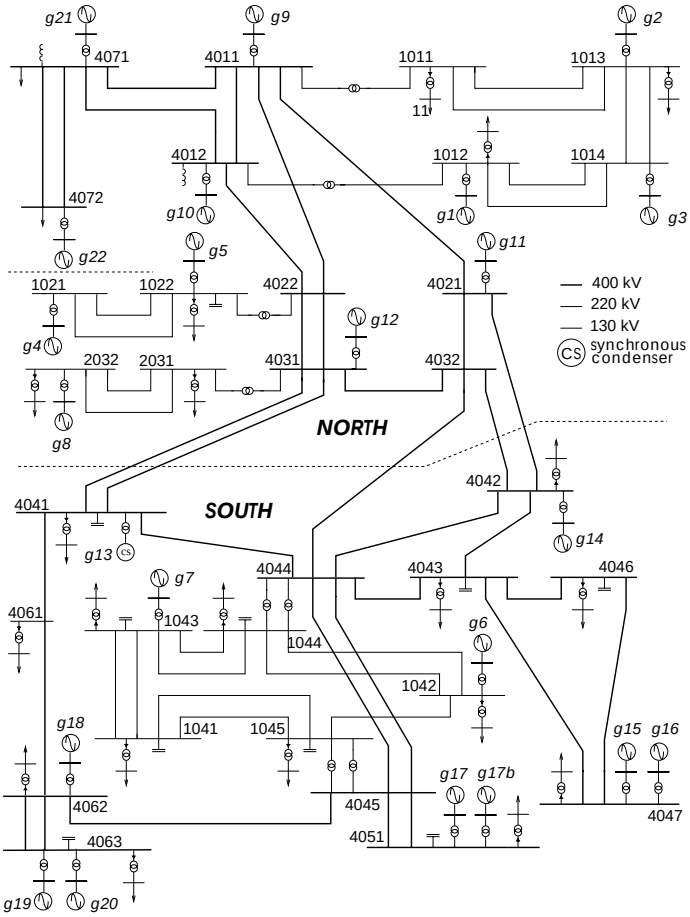


Figure 4: The "Nordic 32" test system

The QSS long-term simulation reproduces the dynamics of Load Tap Changers (LTCs) and OverExcitation Limiters (OELs). Note that there is no slack-bus in the QSS model; instead, generators respond to a disturbance according to governor effects [2]. Moreover, it is assumed that generators of the North area only are under governor control (i.e. the others have infinite speed droops).

The stress of concern is a load increase in the whole system (6 loads in the North, 14 in the South area, with $S_{max} = 1000$ MW/ 300 Mvar) covered by a generation increase in the North area (10 generators, $S_{max} = 1050$ MW, accounting for losses), each according to participation factors.

Figure 5 illustrates the binary search of a limit. It shows the time evolution of a 400-kV bus voltage, under the effect of a contingency applied at $t = 10$ s. The curves relate to four pre-contingency stress levels : 0 (base case), $S_\ell$ (marginally stable), $S_u$ (marginally unstable) and $S_{max}$.

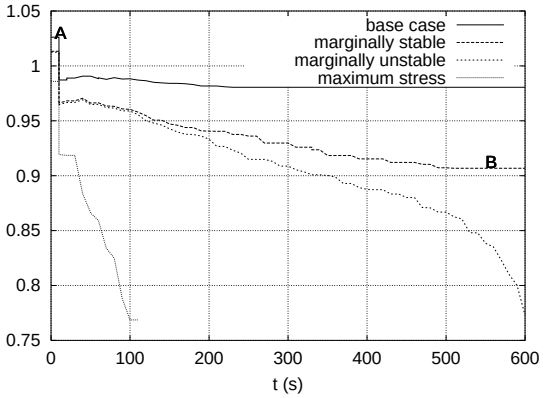


Figure 5: Evolution of a voltage (pu) at 4 steps of a binary search

In this example, the reactive reserves are computed with respect to the risk of voltage instability. Namely, the system response to a contingency is considered acceptable if it is stable; no other operating constraint is added. The $Q^{\star}_{post,\,i}$ generations are thus computed at point B of Fig. 5. The base case generations $Q_{\,i}$ are obviously obtained at point A of the same figure.

We present results relative to five contingencies with different impacts on the system. Table 1 gives the corresponding margins $S^{\star}$, numbers of generators in $\mathcal{E}$, reserves (5, 9) and security indices (11).

Table 1: Nordic 32 system : margins and reserves

| contingency: loss of | $S^{\star}$ (MW) | nb of gen. in $\mathcal{E}$ | $R^{min}$ (Mvar) | $R$ (Mvar) | $\frac{R - R^{min}}{R^{min}}$ |
|---|---|---|---|---|---|
| g17 | 440 | 22 | 2792 | 3943 | 0.41 |
| 4011-4021 | 497 | 22 | 2229 | 3575 | 0.60 |
| 4031-4041 | 668 | 16 | 1092 | 2865 | 1.62 |
| g13 | 893 | 6 | 193 | 1638 | 7.4 |
| g2 | 901 | 5 | 188 | 1398 | 6.4 |

A deeper look into the system behaviour is offered by Fig. 6 which shows for the 23 generators the values of: the base case production $Q^{\,b}_{\,i}$ (in black), $Q^{\star}_{pre,\,i}$ (in dark grey), $Q^{\star}_{post,\,i}$ (in light grey) and $Q^{lim}_{i}$ (in white). We take for the latter the reactive power that the generator produces once under field current limit, its voltage and active production being at their base case values. For legibility purposes, the 802 Mvar limit of (the large) generator g9 is not shown. Similarly, g22 is an equivalent generator with a very large capability, not shown either.

Since we use an accurate QSS simulation instead of a standard load flow with constant reactive limits, it is possible for a generator to have:
• $Q^{\star}_{post,\,i} > Q^{lim}_{i}$ (see e.g. g5 and g7 in Fig. 6). This corresponds to a generator reaching its field current limit in the post-contingency simulation. Once the limit is enforced, the (uncontrolled) terminal voltage decreases, and the reactive production slightly increases above the base case value taken as $Q^{\,lim}_{\,i}$;
• $Q^{\star}_{post,\,i} < Q^{lim}_{i}$ while the generator is field current limited in the post-contingency situation (see e.g. g11 and g12 in Fig. 6). This results from an increase in active power production, due to either the stress or the contingency, causing the reactive power capability to decrease below the base case value.

The results of Fig. 6 illustrate that the effective capability $Q^{\star}_{post,\,i}$ is often significantly lower than the technical limit $Q^{\,lim}_{\,i}$, due to the network inability to transmit reactive power.

The following observations relate to each particular contingency:
• *loss of generator g17*: almost all generators react to the contingency. For instance, setting the $\epsilon$ threshold to 20 Mvar leads to having all generators in $\mathcal{E}$. While the loss of g17 reactive production (55 Mvar) is compensated by the nearest generators (mainly g17b), the loss of its active production (500 MW) has to be balanced by the generators of the North area, the only ones participating to frequency control. The resulting additional power transfer induces high reactive losses which solicit almost all generators;
• *loss of line 4011-4021*: the 636-MW pre-contingency line power flow is redirected into the 4011-4022 and 4011-4012 lines mainly. Expectedly, the corresponding increase in reactive power losses solicit the Northern generators (g9, g10, etc.), as well as the centrally located g13 and g14. The Southern generators react to a much smaller extent;
• *loss of line 4031-4041*: the generator reaction is somewhat less extended with 16 generators in $\mathcal{E}$ instead of 22 in the previous two cases;
• *loss of generator g13*: the loss of this synchronous condenser impacts the reactive power balance only. With 6 generators in $\mathcal{E}$ the disturbance can be considered local. Note that $\mathcal{E}$ is identified at the $S^{\star}$ stress, where the compensator produces 133 Mvar. A similar analysis carried out in the base case, where it absorbs power, would not yield such significant results;
• *loss of generator g2*: although both active and reactive powers are lost, almost no effect is felt by the Southern generators.

Coming back to Table 1, a very good agreement is found between the margin $S^{\star}$ and the security indicator $I$. This can be justified as follows. Consider for instance the last two contingencies, which have a large margin $S^{\star}$. It is thus required to increase the load by a large amount to make these contingencies harmful. The $Q^{\star}_{post,\,i}$ values are thus high and so is the reserve $R$. On the other hand, the individual responses $Q^{\star}_{post,\,i} - Q^{\star}_{pre,\,i}$ to the disturbance are small and so is $R^{min}$.

### *4.2. Examples from the EDF system*

With a peak load of about 75,000 MW, EDF operates a large system from 7 regional and one national control centers. This system is rather dense and meshed. Much attention is paid to

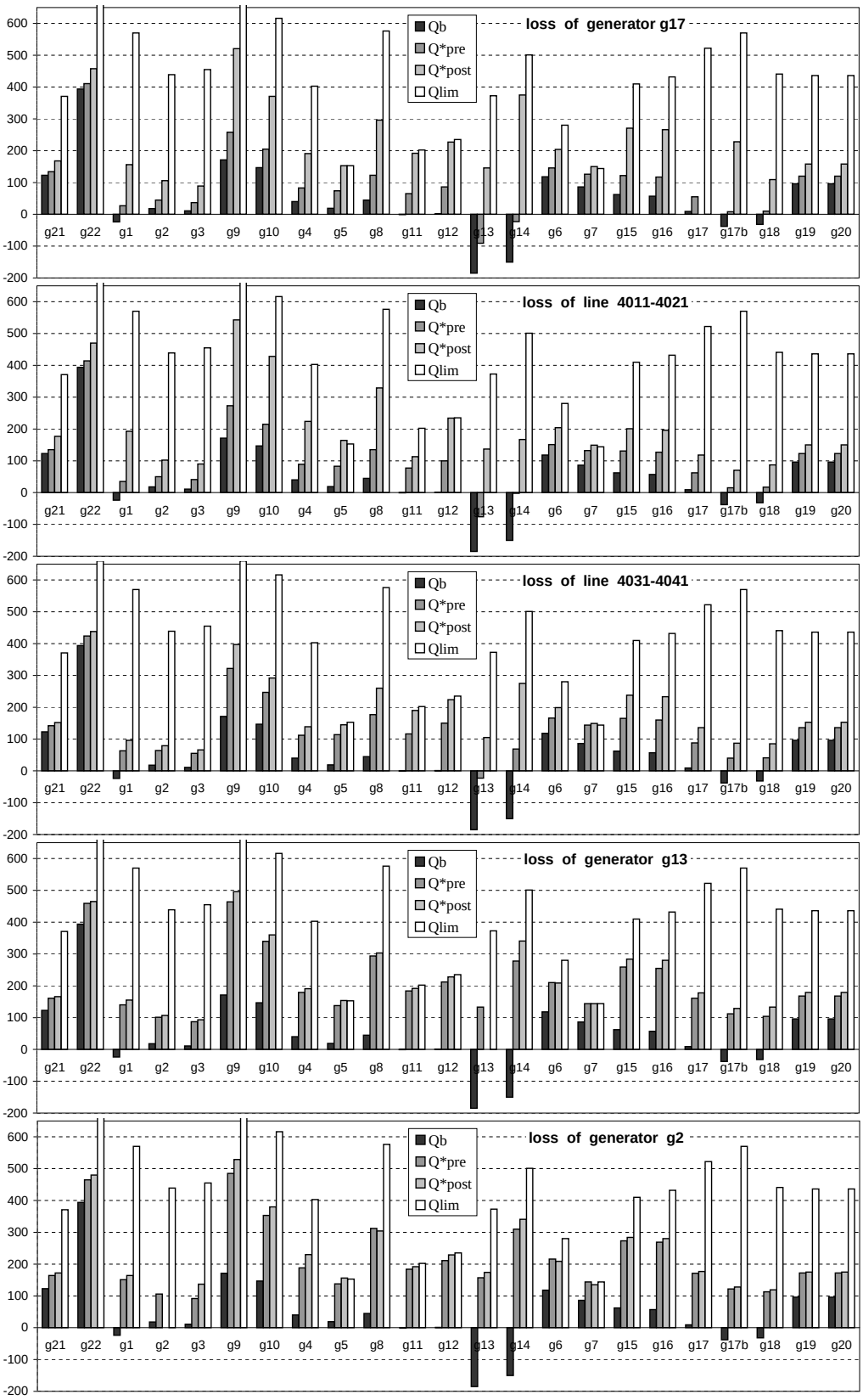


Figure 6: Nordic 32 system : values of $Q_i^b$, $Q_{pre,\,i}^{\star}$, $Q_{post,\,i}^{\star}$ and $Q_i^{lim}$ of all generators

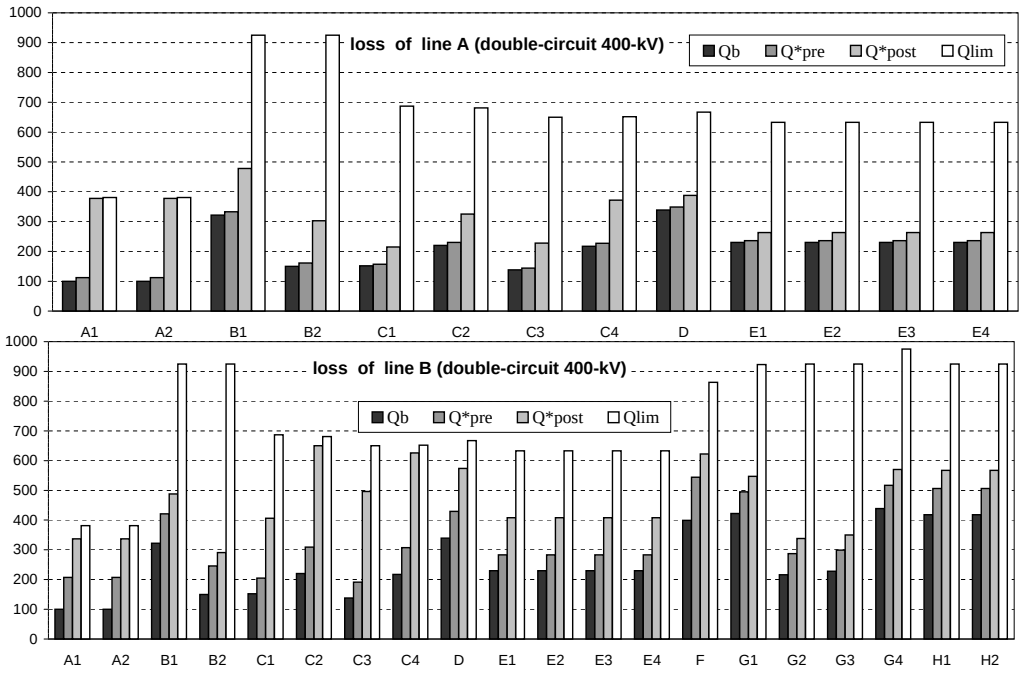


Figure 7: EDF system : values of $Q_i^b$, $Q_{pre,\,i}^{\star}$, $Q_{post,\,i}^{\star}$ and $Q_i^{lim}$ of generators in $\mathcal{E}$

voltage security in the Western and South-East regions.

The QSS simulation model includes 1203 buses at the 400 and 225-kV levels together with 512 intermediate buses in the load equivalents, 1024 LTCs, 176 OELs and 15 secondary voltage controllers in the Western and South-East regions. Each of them controls the voltage of some generators so as to keep the voltage of a pilot bus almost constant and the reactive power production of each generator proportional to its capability. Further information on the system modelling can be found in [9, 10].

We present results relative to two $N-2$ contingencies, namely the tripping, in the Western part of the system, of two double-circuit 400-kV lines, referred to as A and B, respectively.

We first take as system stress a national load increase covered by French generators. Table 2 gives the corresponding margins $S^{\star}$, numbers of generators in $\mathcal{E}$, reserves (5, 9) and security indices (11). The loss of line A is a contingency with local effects, the system becoming voltage unstable in its very Western extremity. The margin is small and so is the index $I$ . The loss of line B has a wider impact but the load must be increased by a much larger amount before this contingency becomes harmful. Expectedly, unlike the small Nordic 32 system, this system has only a small subset of generators involved in each contingency. The more local the contingency, the smaller this subset.

Figure 7, analogous to Fig. 6, relates to generators in $\mathcal{E}$ only ($\epsilon = 20$ Mvar). It confirms that the loss of line A has a more local impact. For both contingencies, generators A1 and A2 are the closest to the tripped lines and are field current limited in

Table 2: EDF system : margins and reserves

| contingency: loss of | $S^{\star}$ (MW) | nb of gen. in $\mathcal{E}$ | $R^{min}$ (Mvar) | $R$ (Mvar) | $\frac{R-R^{min}}{R^{min}}$ |
|---|---|---|---|---|---|
| line A | 490 | 13 | 1350 | 1461 | 0.08 |
| line B | 4142 | 30 | 2897 | 5165 | 0.78 |

the marginally accepted post-contingency situation. Generator B1 (resp. B2) has a large reactive capability but the effective reserve is only one half (resp. one third) of it.

Figures 8 to 10 show how the value of $R$ and $R^{min}$ relative to a given (base case) operating point changes with the direction of stress used to compute them. To this purpose, loads have been increased homothetically in 12 "concentric" areas, all including the area most affected by the contingency. The abscissa in Figs. 8

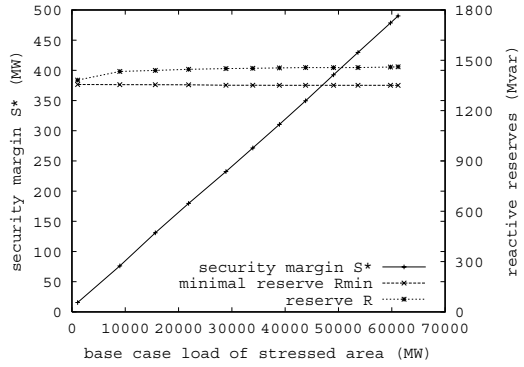


Figure 8: influence of stressed area (EDF system, loss of line A)

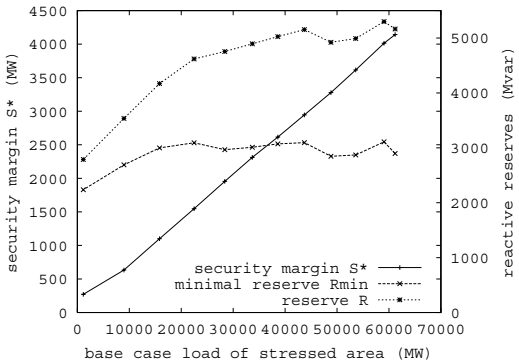


Figure 9: influence of stressed area (EDF system, loss of line B)

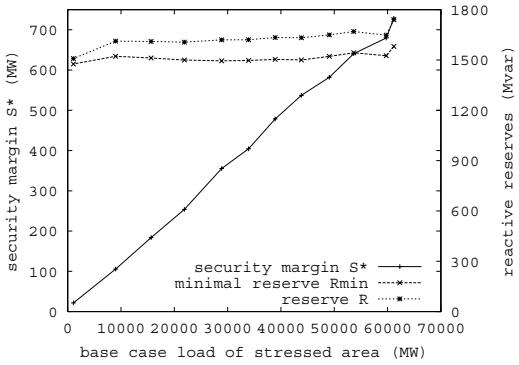


Figure 10: same as Fig. 8 with secondary voltage control

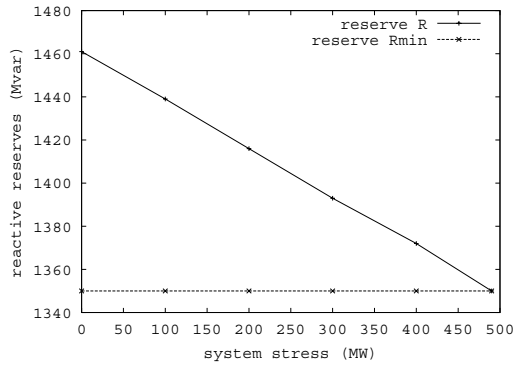


Figure 11: evolution of reserves with stress (EDF system, loss of line A, same stress used to compute reserves)

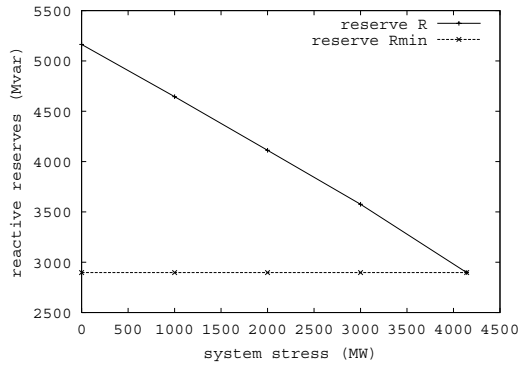


Figure 12: evolution of reserves with stress (EDF system, loss of line B, same stress used to compute reserves)

to 10 is the base case load power consumed in the stressed area. Each figure shows $S^\star$, $R^{min}$ and $R$, respectively.

As can be seen, the security margin $S^\star$ decreases (almost) linearly with the size of the stressed area. The mimimum reserve, on the other hand, remains rather constant, provided that the stressed area does not approach too much the "heart of instability". The invariance of $R^{min}$ for the most dangerous contingency (loss of line A) is noteworthy. The reserves $R$ undergo more important changes, which seem to follow those of $R^{min}$.

Figures 8 and 9 have been obtained in the absence of secondary voltage control. When the latter is in operation, the curves of Fig. 8 become those of Fig. 10. This figure shows the expected improvement in the margin $S^\star$. The security index $I$ is also larger.

Figures 11 to 14 show how the reserves evolve with the system stress. Let us emphasize that in all four figures, a national load increase is assumed to compute $R$ and $R^{min}$ (this corresponds to the rightmost point in Figs. 8 and 9).

In Figs. 11 and 12 the system is stressed along the direction assumed when computing the reserves. As the stress increases, the available reserve $R$ decreases. Due to the way it is computed, the minimal reserve $R^{min}$ remains unchanged. The $R$ and $R^{min}$ curves necessarily intersect at a stress level equal to the margin $S^\star$ given in Table 2. The linear variations of both $R$ and $I$ are noteworthy.

In Figs. 13 and 14, on the other hand, the system is stressed more locally, which yields much smaller margins (37 and 355 MW, respectively). Despite the fact that, at each operating point, $R$ and $R^{min}$ were computed assuming a national load increase, the $R$ and $R^{min}$ curves still intersect at a stress level equal to the margin $S^\star$. The final increase observed in Fig. 14 is due to some generators lately entering the set $\mathcal{E}$ as well as a slightly larger response $Q^\star_{post,\,i} - Q^\star_{pre,\,i}$ to the contingency. The method could still be improved to avoid such variations. Note, however, that the security index $I$ decreases linearly towards zero as the stress approaches the margin $S^\star$.

## 5. Conclusion

The ideas developed in this paper can be summarized as follows:
1. the minimum reactive power reserve $R^{min}$ needed to face a contingency is the total reactive power produced in response to the contingency, when the system has been previously stressed so that its post-contingency operating point is just acceptable;
2. the reactive power produced by a generator at this ultimate post-contingency operating point is taken as the effective capability of this generator, for the contingency of concern. For most generators of a (large enough) system, the effective capability is smaller than the technical one, due to the impossibility of trans-

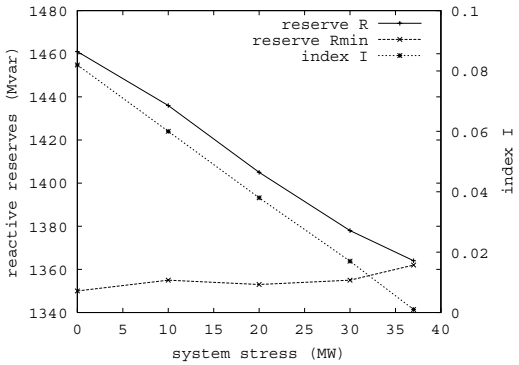


Figure 13: evolution of reserves with stress (EDF system stressed locally, loss of line A)

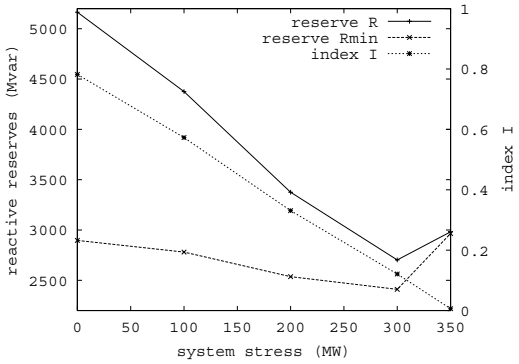


Figure 14: evolution of reserves with stress (EDF system stressed locally, loss of line B)

mitting reactive power over long distances;
3. at a given pre-disturbance operating point, the reactive reserve $R$ available to face the contingency is a sum of differences between the effective capability and the current production. This sum extends over the set $\mathcal{E}$ of generators responding significantly to the contingency;
4. the ratio $(R - R^{min})/R^{min}$ is a convenient, dimensionless security index.

The maximum pre-contingency stress mentioned under item 1 can be obtained using a simple binary search coupled with a contingency evaluation method. If such a binary search is already used to compute the secure operation limit with respect to the contingency, the above reactive reserves are obtained at no additional cost.

Although the proposed method can be used in any context where it makes sense to compute reactive power reserves, the paper focused on voltage instability. Encouraging results obtained on a small test and a large real-life system have been reported.

There is some dependency of the so obtained reactive reserves on the direction of stress used to compute them. However, the results presented in this paper tend to show that, up to some point, the minimum reserve is rather insensitive to the above choice. Also, even if the system is stressed along another direction than the one assumed to compute the reserves, the difference $R - R^{min}$ between the current and the minimal reserves - and hence the $I$ index - decreases towards zero as the system approaches an operating point where the contingency becomes harmful. A linear decrease has been observed in many cases.

Whereas the key role of reactive reserves is to support the voltage profile in response to contingencies and stress, and thereby contribute to system security, the concepts summarized under items 1 to 3 above constitute a basis for the valuation of reactive reserves. With respect to a single contingency, it sounds reasonable to reward a generator up to the amount corresponding to its effective capability (see item 2). To take the whole set of credible contingencies into account, one could either consider the maximum effective capability over all scenarios or a weighted sum cumulating the effects of the various contingencies.

**Acknowledgement**. We thank Electricité de France for allowing us to use its data and publish the corresponding results.

**References**

[1] C. W. Taylor, *Power System Voltage Stability*, McGraw Hill, EPRI Power System Engineering Series, 1994

[2] T. Van Cutsem, C. Vournas, *Voltage Stability of Electric Power Systems*, Kluwer Academic Publisher, 1998

[3] B. Avramovic and L. H. Fink, "Real-time Reactive Security Monitoring", IEEE Trans. on Power Systems, Vol. 7, 1992, pp. 432-437

[4] R. A. Schlueter, I. Hu, M.W. Chang, J.C. Lo, A. Costi, "Methods for determining proximity to voltage collapse", IEEE Trans. on Power Systems, Vol. 6, Feb. 1991, pp. 285-292

[5] R. A. Schlueter, "A Voltage Stability Security Assessment Method", IEEE Trans. on Power Systems, Vol. 13, 1998, pp. 1423-1438

[6] C.W. Taylor and R. Ramanathan, "BPA Reactive Power Monitoring and Control following the August 10, 1996 Power Failure", Proc. VIth SEPOPE conference, Salvador (Brazil), May 1998, paper IP-003

[7] W. Xu, Y. Zhang, L.C.P. da Silva, P. Kundur, "Competitive Procurement of Dynamic Reactive Power Support Service for Transmission Access", Proc. IEEE PES Summer Meeting, July 2000, Vol. 1, pp. 543-548

[8] T. Van Cutsem, C. Moisse, R. Mailhot, "Determination of secure operating limits wih respect to voltage collapse", IEEE Trans. on Power Systems, vol. 14, 1999, pp. 327-335

[9] T. Van Cutsem, F. Capitanescu, C. Moors, D. Lefebvre, V. Sermanson, "An advanced tool for preventive voltage security assessment", Proc. VIIth SEPOPE conference, Curitiba (Brazil), 2000, paper IP-035

[10] V. Sermanson, C. Moisse, T. Van Cutsem, Y. Jacquemart, "Voltage security assessment of systems with multiple instability modes", Proc. Bulk Power System Dynamics and Control V, Santorini, Greece, Aug. 1998, pp. 185-196